Available online at www.sciencedirect.com
ScienceDirect
Polymer 48 (2007) 2312–2321
polymer
www.elsevier.com/locate/polymer

A pH-sensitive double [60]fullerene-end-capped polymers via ATRP: Synthesis and aggregation behavior

H. Yu [a], L.H. Gan [a,*], X. Hu [b], Y.Y. Gan [a]

[a] *Natural Sciences and Science Education, National Institute of Education, Nanyang Technological University, 1 Nanyang Walk, Singapore 637616, Republic of Singapore*

[b] *School of Materials Science and Engineering, Nanyang Technological University, 1 Nanyang Walk, Singapore 637616, Republic of Singapore*

Received 5 May 2006; received in revised form 13 February 2007; accepted 19 February 2007
Available online 22 February 2007

Abstract

A double [60]fullerene (C_{60})-end-capped water-soluble polymer [C_{60}-DMAEMA$_{68}$-C(CH$_3$)$_2$COOCH$_2$]$_2$ was synthesized by cycloaddition of the double azido-terminated [DMAEMA$_{68}$-C(CH$_3$)$_2$COOCH$_2$]$_2$ with C_{60}. The well-defined [Br(Cl)-DMAEMA$_{68}$-C(CH$_3$)$_2$COOCH$_2$]$_2$ was first synthesized via ATRP using ethylene bis(2-bromoisobutyrate) as initiator in ethanol. TGA and spectrophotometric analyses confirmed that mono-addition to C_{60} had occurred. In aqueous solution, [C_{60}-DMAEMA$_{68}$-C(CH$_3$)$_2$COOCH$_2$]$_2$ self-assembled into flower micelles. The aggregation behaviors in unbuffered distilled water and in acidic solution at pH 3 were studied by laser light scattering (LLS). The micelles formed in distilled water has an aggregation number (N_{agg}) of ~242 which is about three times larger than that at pH 3 solution ($N_{agg} = 81$). However, the micellar size is bigger at pH 3, due to the highly stretched corona resulting from the charge repulsion among the protonated amino groups. After calcination, the C_{60} core could be seen clearly by AFM. The critical micelle concentration (CMC) of [C_{60}-DMAEMA$_{68}$-C(CH$_3$)$_2$COOCH$_2$]$_2$ is lower in unbuffered distilled water (28.6 mg dm^{-3}) than in solution at pH 3 (176.8 mg dm^{-3}).

Keywords: Amphiphilic polymeric [60]fullerene; Flower micelles; Poly(DMAEMA)

1. Introduction

[60]Fullerene (C_{60}) has been a subject of intense research due to its unique structure, interesting properties and many potential applications [1–4] ever since it was discovered in 1985. More recently, considerable efforts have been directed toward the syntheses of well-defined C_{60}-containing polymers, in particular via atom transfer radical polymerization (ATRP) method. C_{60}-containing polymers with well-defined structure and low polydispersity indexes are particularly desirable in the study of the aggregation behavior as more uniform aggregates could be obtained.

ATRP [5] is a convenient technique to prepare polymers with low polydispersity and carrying terminal functional groups. Typically, the end group is either bromine or chlorine which can be coupled to C_{60} directly [6] or via azido addition [7,8]. Recent reports on the ATRP of well-defined single C_{60}-end-capped polymers include PSt-C_{60}, PMMA-C_{60} by Li et al. [6,7], P*t*BA-C_{60} by Yang et al. [8] and PDMAEMA-C_{60}, PtBMA-C_{60}, PMAA-C_{60} by Tam et al. [9–11] Double C_{60}-end-capped polymers have also been reported. Song et al. [12] synthesized C_{60}-PEO-C_{60} and its aggregation behavior in THF and water was studied. Yu et al. [13] reported the synthesis of well-defined double C_{60}-end-capped triblock copolymer C_{60}-DMAEMA-*b*-PEO-*b*-DMAEMA-C_{60}. Various C_{60}-PEO-C_{60} samples of different PEO chain lengths are reported to form pseudo-semi-interpenetrating polymer networks (pseudo-SIPNs) after melt blended with PMMA. The pseudo-SIPNs exhibited remarkable enhancement in mechanical properties. The storage modulus of one particular sample (FPEO12F) showed a 16 times increase over PMMA [14]. In solutions, C_{60}-PEO-C_{60} (453 EO units) aggregates into simple spherical micelles in THF, but in

* Corresponding author. Tel.: +65 67903811; fax: +65 68969414.
E-mail address: leonghuat.gan@nie.edu.sg (L.H. Gan).

0032-3861/$ - see front matter © 2007 Elsevier Ltd. All rights reserved.
doi:10.1016/j.polymer.2007.02.050

aqueous solution, only network structure was observed [12]. In contrast, we have earlier reported for the first time that a C_{60}-containing polymer (C_{60}-DMAEMA$_{60}$-*b*-PEO$_{105}$-*b*-DMAEMA$_{60}$-C_{60}) forms exclusively well-defined uniform micelles in aqueous solutions [13]. Poly[2-(dimethylamino)ethyl methacrylate (PDMAEMA) is a water-soluble and pH-sensitive polymer. C_{60}-PDMAEMA synthesized via ATRP was soluble in water and formed micellar aggregates at pH < 7.2. However, substantial proportion of the polymers also coexisted as unimers, suggesting that the micelles of the single C_{60}-end-capped PDMAEMA were not particularly stable [9]. In this paper, we report the aggregation behavior of a double C_{60}-end-capped PDMAEMA in aqueous solution. The polymer forms well-defined micelles in acidic and near neutral solutions with no detectable presence of the unimers.

2. Experimental

2.1. Materials

2-(Dimethylamino)ethyl methacrylate (DMAEMA, 99%, Merck) was purified by passing through an alumina column and distilled prior to use. C_{60} (99.5%) was purchased from SES Research (USA). Ethylene glycol (99.5%) was purchased from Merck. 2-Bromoisobutyryl bromide (98%), copper(I) chloride (CuCl, 99.5%), and sodium azide (99%) were purchased from Aldrich. 1,1,4,7,10,10-Hexamethyl triethylene tetramine (HMTETA, 97%) was purchased from Acros. Ethanol was dried by magnesium and distilled. Tetrahydrofuran (THF), dimethylformamide (DMF) and 1,2-dichlorobenzene were dried by CaH_2 and distilled.

2.2. Synthesis

2.2.1. Ethylene bis(2-bromoisobutyrate) (EBBIB) (*I*)

A solution of 2-bromoisobutyryl bromide (13.2 mL, 0.107 mol) in 20 mL $CHCl_3$ at 0 °C was added dropwise to a 250 mL round-bottomed flask containing $CHCl_3$ (50 mL), ethylene glycol (2.0 mL, 0.0357 mol), and triethylamine (14.9 mL, 0.107 mol) also maintained at 0 °C in an ice-bath. The reaction mixture was stirred at 25 °C for 24 h, after which 100 mL of distilled water was added. The solution was then transferred to a 250 mL separating funnel. The $CHCl_3$ phase was retained, washed by 25 mL each of distilled water three times, dried by Na_2SO_4 and filtered. The filtrate was collected and concentrated using a rotary evaporator. The residue was vacuum distilled and the product was collected at 106–108 °C/3 mbar. The yield was 9.2 g (71.4%). ^{1}H NMR ($CDCl_3$) δ (ppm): 4.31–3.89 (t, $-OCH_2CH_2O-$), 1.94 (s, $-CH_3$).

2.2.2. [Br(Cl)-DMAEMA$_{68}$-C(CH$_3$)$_2$COOCH$_2$]$_2$ (*II*)

The polymerization of DMAEMA through the extension from both ends of EBBIB in alcoholic solvent was performed via the ATRP technique according to the procedure described by Mao et al. [15]. CuCl (0.016 g, 0.162 mmol) was added to a dry 25 mL Schlenk flask with a magnetic stirring bar. The Schlenk flask was evacuated and flushed with argon. DMAEMA (3.0 mL, 18.0 mmol), HMTETA (0.044 mL, 0.162 mmol), and degassed ethanol (3.0 mL) were added using separate Ar-purged syringes. The mixture was stirred for 10 min and degassed by three freeze-pump–thaw cycles. The flask was then placed in a water bath maintained at 25 ± 0.2 °C. Finally, EBBIB (19 μL, 0.081 mmol) was added using an Ar-purged syringe. After stirring for 6 h, the reaction was terminated by the addition of THF (20 mL). The solution was then passed through a basic alumina column to remove the catalyst. [Br(Cl)-DMAEMA$_{68}$-C(CH$_3$)$_2$COOCH$_2$]$_2$ was obtained by precipitation into 20-fold of hexane. The product was isolated and dried under vacuum. The yield was 2.55 g (equivalent to 90.0% conversion of monomer), M_n = 21,600 and PDI = 1.22. ^{1}H NMR ($CDCl_3$) δ (ppm): 4.28 (s, $-OCH_2CH_2O-$), 4.05 (s, $-OCH_2CH_2N<$), 2.60 (s, $>NCH_2-$), 2.40 (s, $>NCH_3$), ~1.90 (m, $-C-CH_2-$), and 1.1–0.90 (d, $-C-CH_3$).

2.2.3. [N$_3$-DMAEMA$_{68}$-C(CH$_3$)$_2$COOCH$_2$]$_2$ (*III*)

A 25 mL DMF solution containing NaN_3 (22.0 mg) and (**II**) (2.40 g) was added to a 50 mL round-bottomed flask. The mixture was allowed to react with stirring at 25 °C overnight after which the solvent was removed almost completely under reduced pressure, and the residue was redissolved in 10 mL of THF. The solution was filtered to remove excess NaN_3. The filtrate, after reduced to a volume of ~2 mL by rotary evaporation, was added to 50 mL hexane for precipitation. The precipitate was filtered, washed by hexane and dried under vacuum at 25 °C. The yield was 1.8 g (75.0 wt%). ^{1}H NMR ($CDCl_3$) δ (ppm): 4.28 (s, $-OCH_2CH_2O-$), 4.05 (s, $-OCH_2CH_2N<$), 2.60 (s, $>NCH_2-$), 2.40 (s, $>NCH_3$), ~1.90 (m, $-C-CH_2-$), and 1.1–0.90 (d, $-C-CH_3$).

2.2.4. [C$_{60}$-DMAEMA$_{68}$-C(CH$_3$)$_2$COOCH$_2$]$_2$ (*IV*)

A 50 mL round-bottomed flask equipped with a spiral condenser was charged with (**III**) (1.70 g), C_{60} (147.0 mg) and 1,2-dichlorobenzene (20 mL). The flask was immersed in an oil bath maintained at 130 °C under argon atmosphere. After refluxing for 48 h, the solvent was removed by rotary evaporation. THF (5 mL) was then added and the excess C_{60}, which was insoluble in THF, was separated by centrifugation. The supernatant was withdrawn and precipitated into 100 mL hexane. The brownish product of [C_{60}-DMAEMA$_{68}$-C(CH$_3$)$_2$COOCH$_2$]$_2$ was filtered, washed and dried under vacuum at 60 °C. The yield was 1.5 g (83.0 wt%). ^{1}H NMR ($CDCl_3$) δ (ppm): 4.28 (s, $-OCH_2CH_2O-$), 4.05 (s, $-OCH_2CH_2N<$), 2.60 (s, $>NCH_2-$), 2.40 (s, $>NCH_3$), ~1.90 (m, $-C-CH_2-$), and 1.1–0.90 (d, $-C-CH_3$).

2.3. Characterization

FT-IR spectra were recorded on a Perkin–Elmer FT-IR spectrometer. Thermogravimetric measurements were conducted with a Perkin–Elmer Pyris 1 TGA Thermogravimetric Analyzer. Approximately 6 mg of sample was heated at a rate of 20 °C/min from 30 °C to 1000 °C in a dynamic nitrogen atmosphere (flow rate = 50 mL/min). A HP8453 UV–visible spectrophotometer equipped with a HP89090A temperature

control unit was used for UV–visible absorption measurements. ^{1}H NMR spectra were recorded on a Bruker DRX 400 spectrometer in $CDCl_3$. Surface tension measurements were conducted using a KRUSS Tensiometer K100 via ring method. For each concentration, five measurements were performed and the average value was used.

2.4. Laser light scattering (LLS) measurements

A Brookhaven laser light scattering system was used. The system consists of a BI-200SM goniometer, a BI-9000AT digital correlator, and other supporting data acquisition and analysis software and accessories. An argon ion vertically polarized 488 nm laser was used as the light source. The temperature was controlled at 25 ± 0.1 °C using a Science/Electronic water bath. The refractive index increment dn/dC was measured by a BI-DNDC differential refractometer. For dynamic light scattering (DLS) studies, the time correlation function of the scattered intensity $G_2(t)$, defined as $G_2(t) = T(t)I(t + \Delta t)$ where $I(t)$ is the intensity at time t and Δt is the lag time, was analyzed using the inverse Laplace Transformation technique (REPES) to produce the distribution function of decay times. The sample solutions were prepared by dissolving the polymer in MilliQ water, followed by filtration through a 200 μm filter. The concentration range of the polymer solutions was 0.1–1.0 mg mL^{-1}, which is in the dilute solution regime where the behavior of individual particles can be characterized.

2.5. Gel permeation chromatography (GPC)

The molecular weight and molecular weight distribution of polymers were determined by gel permeation chromatography (GPC). An Agilent 1100 series GPC system equipped with a LC pump, PLgel 5 μm MIXED-C column, and RI and UV detectors were used. The column was calibrated with narrow molecular weight distribution polystyrene standards. HPLC grade THF stabilized with 2,6-di-*tert*-butyl-4-methylphenol (BHT) was used as a mobile phase. The flow rate was maintained at 1.0 mL/min. The RI and UV detectors and column were thermostated at 25 °C.

2.6. Atomic force microscopy (AFM)

AFM micrographs were obtained using a Dimension 3100 Atomic Force Microscope, Digital Instrument, Santa Barbara, California under ambient conditions. AFM was operated in the tapping mode with an optical readout using Si cantilevers.

3. Results and discussion

3.1. Synthesis

The synthetic route for the C_{60}-containing polymer is shown in Scheme 1. The GPC curves for the polymerization in ethanol show the molecular weight increases smoothly with reaction time (Fig. 1). The corresponding M_n and PDI version % conversion plots are shown in Fig. 2. A linear relationship between $M_{n,GPC}$ versus % conversion (up to ~90%) indicates that the reaction was under controlled/''living'' conditions. This is further supported by the linear first-order kinetic plot as shown in Fig. 3. The results indicate that (**I**) was an efficient initiator for the system, and that the number of active chains remained nearly constant during the polymerization process. Polymer **II** ($M_{n,GPC}$ 21,600 and PDI 1.22) was used for the subsequently synthesis of (**III**) and (**IV**). Characterizations of the polymers by NMR, FT-IR and GPC are given in Supplementary data.

3.2. TGA

The decomposition thermograms under nitrogen atmosphere are shown in Fig. 4. Both (**II**) and (**IV**) exhibited a distinct decomposition step which occurred at around 350 °C. As in our previous works [13], on the basis of the % weight change, the first decomposition steps of curves a and b are attributed to the loss of $-CH_2CH_2N(CH_3)_2$ fragments from the polymers. The % weight losses agree reasonably well with the calculated values based on the molecular formulae of the two polymers (Table 1). There were residue masses in the thermograms of both (**II**) and (**IV**). The residues are likely due to the formation of some cross-linked networks which were thermally stable at this temperature range. As C_{60} is thermally stable up to 600 °C [16], the % weight of C_{60} in (**IV**) can be calculated by subtracting the residue mass of (**II**) from the mass remained at the second inflexion point of (**IV**) at 480.7 °C. The procedure is based on the assumption that other than C_{60} and Br(Cl) at the chain ends, the residue masses of (**II**) and (**IV**) should be the same as they have identical chemical compositions. The % weight of C_{60} thus obtained was 6.86, agreeing reasonably well with the calculated value of 6.26 wt% based on the chemical formula of (**IV**).

3.3. Lower critical solution temperature (LCST)

Poly(DMAEMA) is a thermal sensitive polymer which exhibits LCST (at ~45 °C) [9] in unbuffered distilled water. (**IV**) also exhibited the thermally induced chain-to-globule transition phenomenon. The plot of % transmittance, measured at $\lambda = 600$ nm as a function of temperature for 0.6 mg mL^{-1} solutions of (**II**) and (**IV**) are shown in Fig. 5. The LCST obtained from the 1st derivative of the % transmittance–temperature plot of (**IV**) was 55.5 °C. This is only slightly higher than the LCST of (**II**) which occurred at 52.1 °C, showing that end-capping of C_{60} has little effect on the LCST.

3.4. Surface tension measurements

The plots of surface tension against the concentration of (**IV**) are shown in Fig. 6, yielding CMC $= 28.6 \times 10^{-3}$ g dm^{-3} and $\gamma_{cmc} = 49.3$ mN m^{-1} in unbuffered distilled water and CMC $= 176.8 \times 10^{-3}$ g dm^{-3} and $\gamma_{cmc} = 57.3$ mN m^{-1} at pH 3. At pH 3, the CMC and γ_{cmc} are higher than the corresponding values in unbuffered distilled water due to repulsion among the positively charged polymer chains.

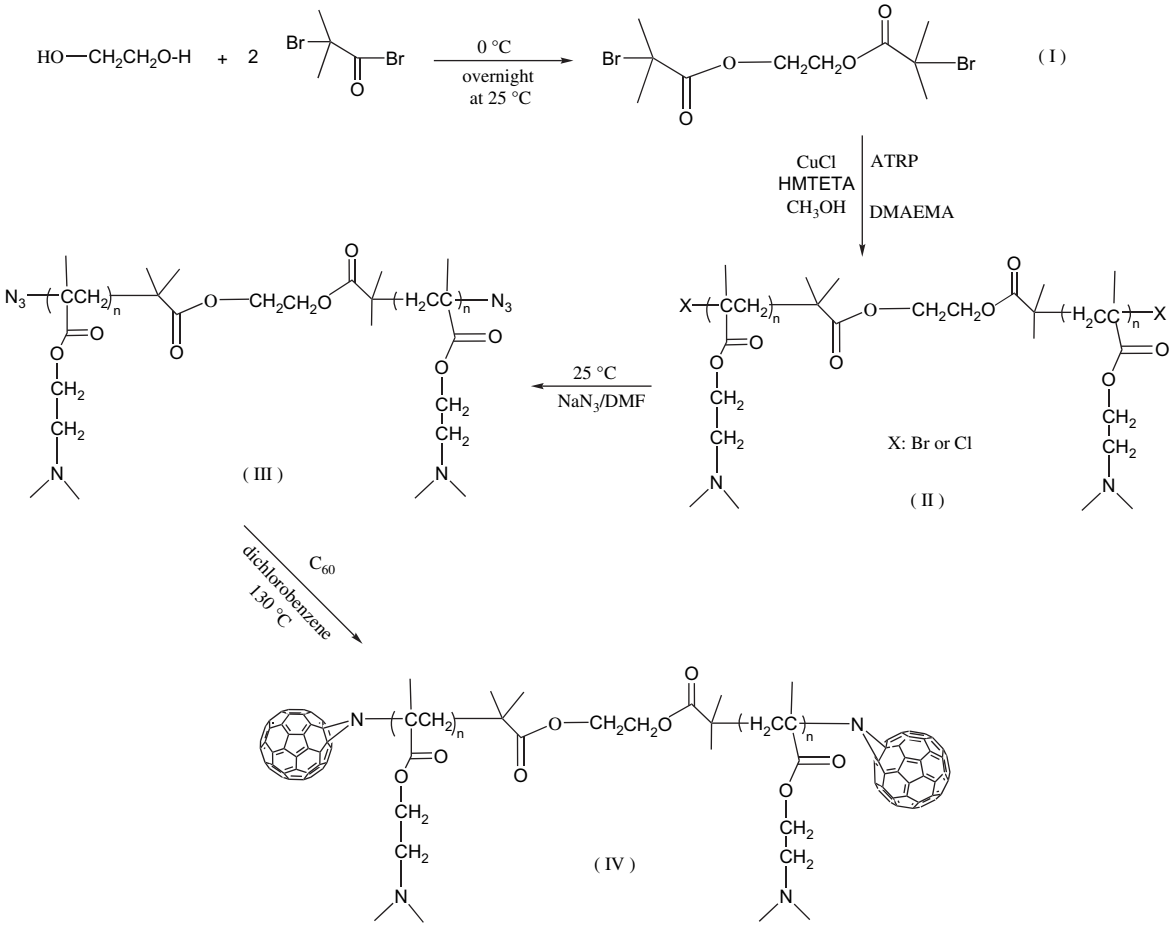

Scheme 1. The synthetic route of $[C_{60}\text{-DMAEMA}_n\text{-C(CH}_3)_2\text{COOCH}_2]_2$.

3.5. Dynamic light scattering

Dynamic light scattering (DLS) measures the intensity fluctuations with time and correlates these fluctuations to the properties of the scattering objects. In general, the terms of correlation functions of dynamic variables are always used to describe the response of the scattering molecules to the incident light. The decay rate Γ, which is the inverse of the relaxation time, τ, is related to the translational diffusion coefficient D by the following expression:

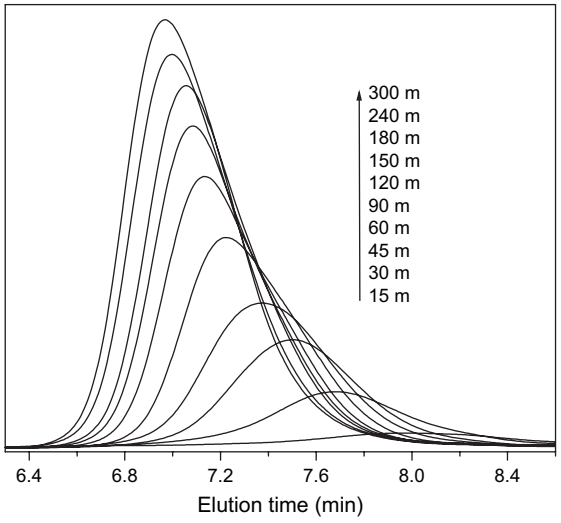

Fig. 1. GPC curves of (**II**) in 50 vol% ethanol at various reaction times. $[CuCl]_0 = [HMTETA]_0 = 0.162$ mmol, $[EBBIB]_0 = 0.081$ mmol, $[DMAEMA]_0 = 11.8$ mmol, and $T = 25$ °C.

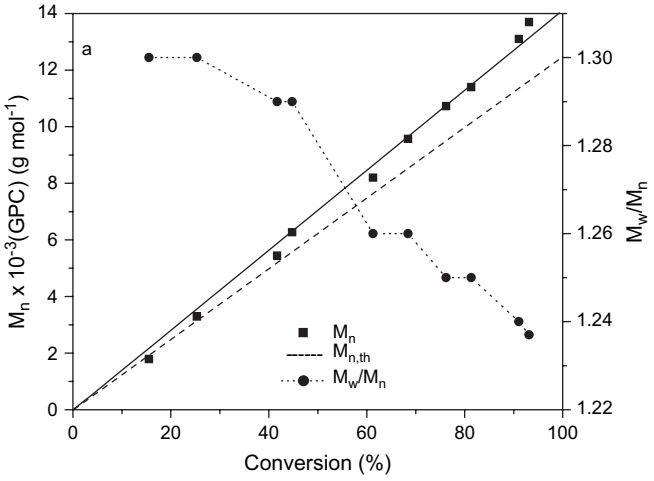

Fig. 2. Evolution of experimental molecular weight and polydispersity with conversion in 50% (v/v) ethanol at $T = 25$ °C. $[CuCl]_0 = [HMTETA]_0 = 0.162$ mmol, $[EBBIB]_0 = 0.081$ mmol, $[DMAEMA]_0 = 11.8$ mmol.

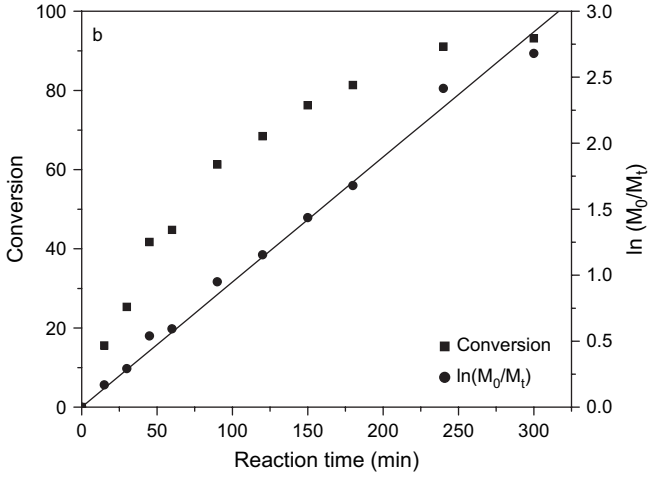

Fig. 3. Semilogarithmic kinetic and conversion plot for ATRP of DMAEMA in 50% (v/v) ethanol at $T = 25\ ^{\circ}C$. $[CuCl]_0 = [HMTETA]_0 = 0.162$ mmol, $[EBBIB]_0 = 0.081$ mmol, $[DMAEMA]_0 = 11.8$ mmol.

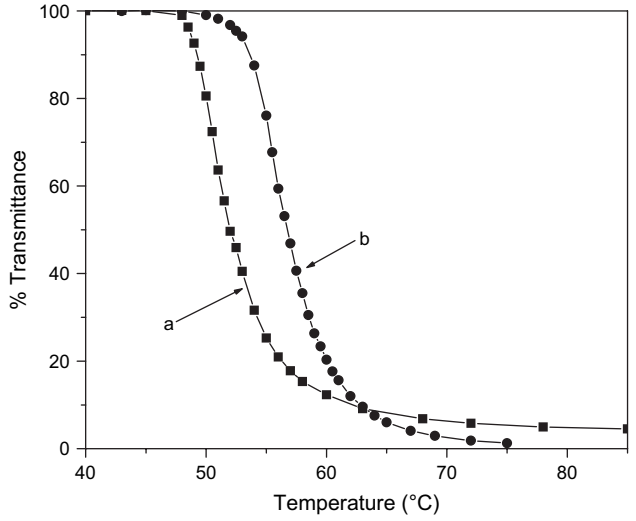

Fig. 5. Plots of % transmittance as a function of temperature of 0.6 mg mL^{-1} aqueous solution of: (a) **II** and (b) **IV**.

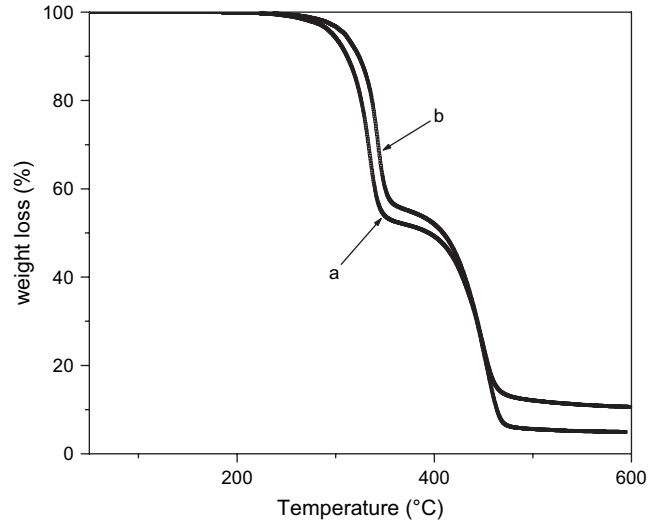

Fig. 4. TGA thermograms of: (a) **II** and (b) **IV**.

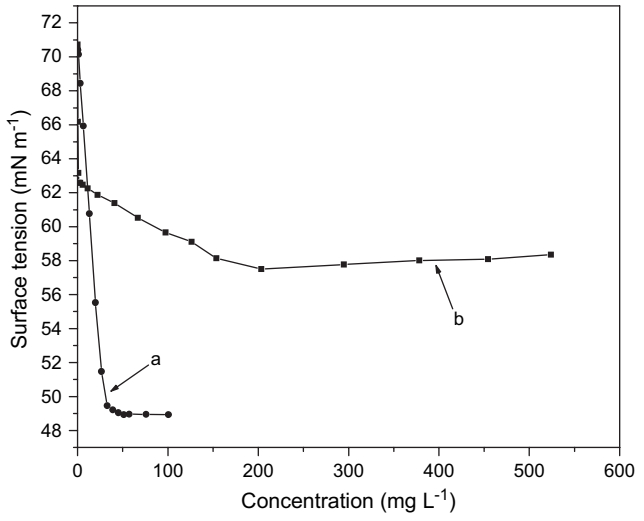

Fig. 6. Plots of surface tension versus concentration of **IV**: (a) at 20 °C in unbuffered distilled water and (b) at pH 3.

Table 1
TGA results of (**II**) and (**IV**)

Polymers	T at 1st inflexion point (°C)	wt% remaining	T at 2nd inflexion point (°C)	wt% remaining	wt% of C_{60}
(**II**)	351.1	53.0 (54.2)[a]	475.3	6.13	
(**IV**)	359.5	56.1 (55.9)[a]	480.7	12.6	6.9 (6.3)[b]

[a] Calculated based on loss of $-CH_2CH_2N(CH_3)_2$.
[b] Calculated based on the chemical formula of **IV**.

$$\Gamma = Dq^2 = D_0q^2(1 + k_dC)\left(1 + f\left\langle R_g^2\right\rangle q^2\right)$$

where q is the scattering vector, expressed as $q = [4\pi n \sin(\theta/2)]/\lambda$, where θ is the scattering angle, n is the refractive index of the solution, and λ is the wavelength of the incident light, D_0 is the translational diffusion coefficients at infinite dilution, f is a dimensionless constant depending on the chain structure, solvent quality, and polydispersity; and k_d is the diffusion second virial coefficient which is the difference between the thermodynamic term ($2A_2M_w$) and the hydrodynamic term ($C_D\langle R_h\rangle^3/M_w$), i.e. $k_d = 2A_2M_w - C_D\langle R_h\rangle^3/M_w$. For a positive k_d, D should increase as C increases.

If the Stokes–Einstein equation is used, the apparent hydrodynamic radius, R_h, can be calculated using the following equation:

$$R_h = \frac{kT}{6\pi\eta D_0}$$

where k is the Boltzmann constant; T is the absolute temperature; and η is the solvent viscosity.

The relaxation time distribution function of (**IV**) in unbuffered distilled water and pH 3 solution at different scattering

angles are shown in Fig. 7(a) and (b), respectively. Only one decay mode was observed in the decay time distribution. The peak relaxation times shifted to lower values with increasing angles, suggesting that only one type of particles was present. The relaxation rate Γ is linearly related to the square of the scattering vector (q^2) as shown in Fig. 8, confirming that the decay mode is due to the translational diffusion of the scattering object. The relaxation time distribution is dependent on the concentration under both conditions (Fig. 9(a) and (b)). The plots of D against the concentration of (**IV**) in unbuffered distilled water and at pH 3 are shown in Fig. 10(a) and (b), respectively. In unbuffered distilled water, the k_d is positive because of larger value of M_w (see results later). Thus D increases with increasing concentration. At pH 3, the repulsion among the positive charges on the polymeric chains caused the polymeric chains to stretch, thus increasing the value of R_h. This sample has smaller M_w, so $2A_2M_w < C_D\langle R_h\rangle^3/M_w$, and k_d is negative. The intercepts yields $D_0 = 8.0 \times 10^{-12}$ m^2 s^{-1}

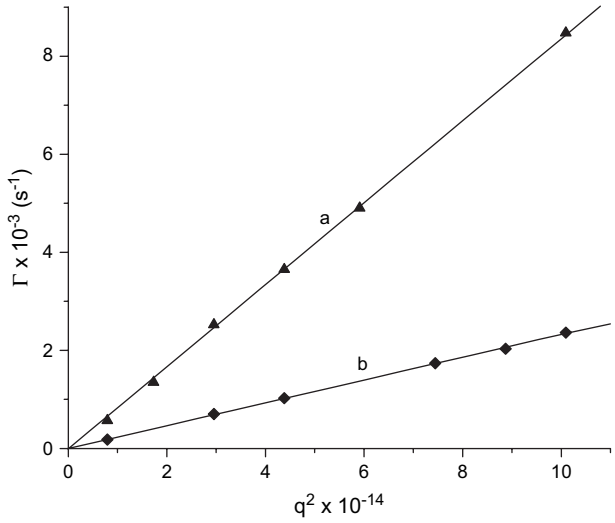

Fig. 8. Plots of Γ versus q^2 of **IV** at 25 °C for: (a) 0.10 mg mL^{-1} in unbuffered distilled water and (b) 0.88 mg mL^{-1} in pH 3.

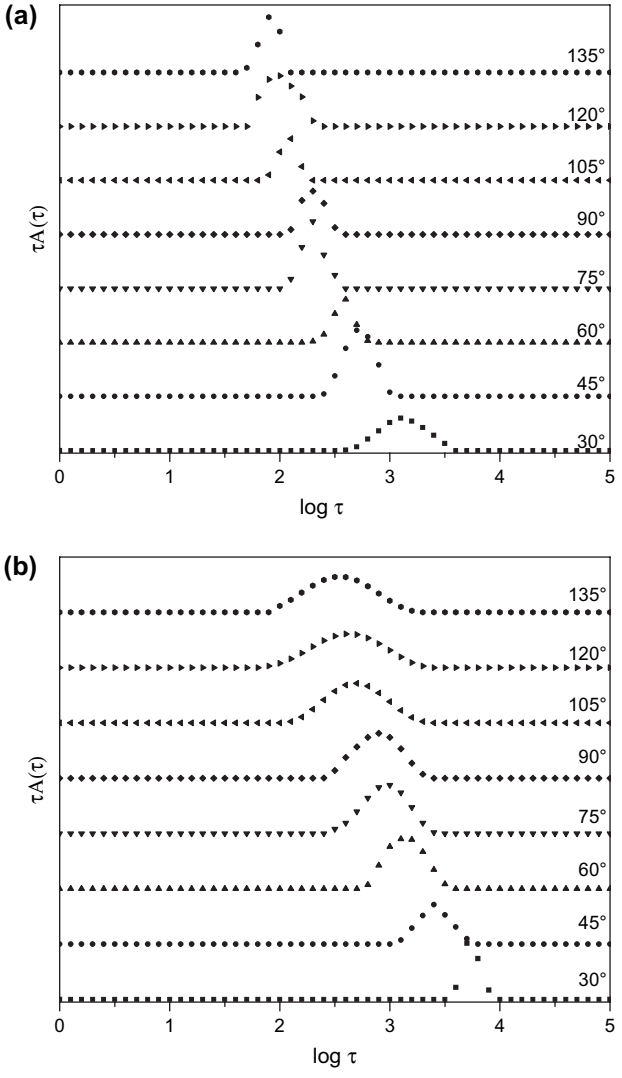

Fig. 7. Decay time distribution function of **IV** at different scattering angles at 25 °C: (a) 0.60 mg mL^{-1} in unbuffered distilled water and (b) 0.88 mg mL^{-1} at pH 3.

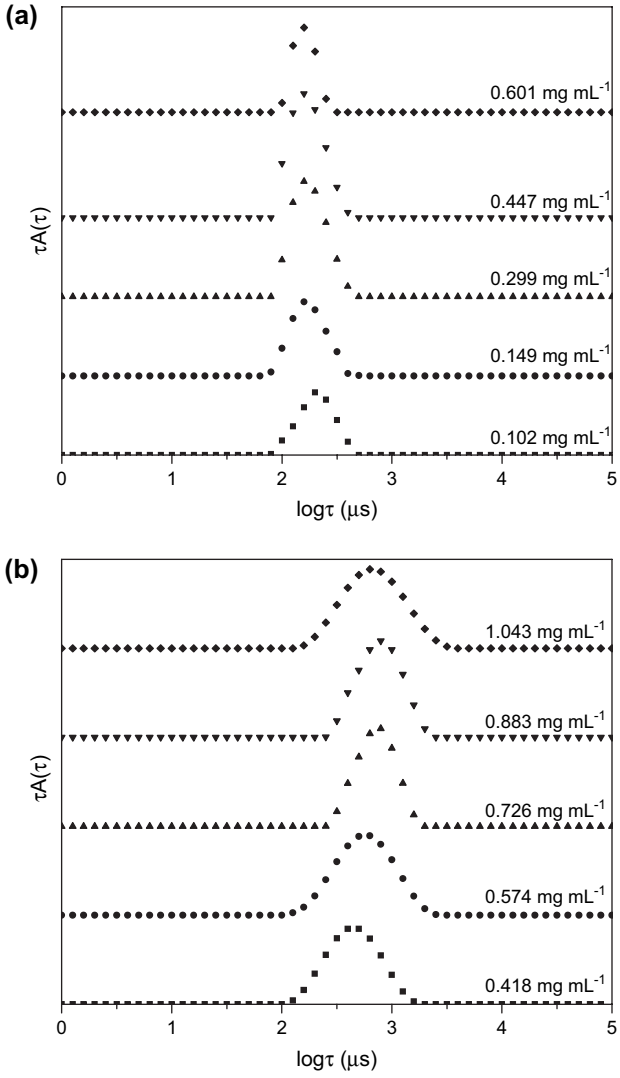

Fig. 9. Decay time distribution functions of (**IV**) at various concentrations of 90° angle at 25 °C: (a) unbuffered distilled water and (b) pH 3.

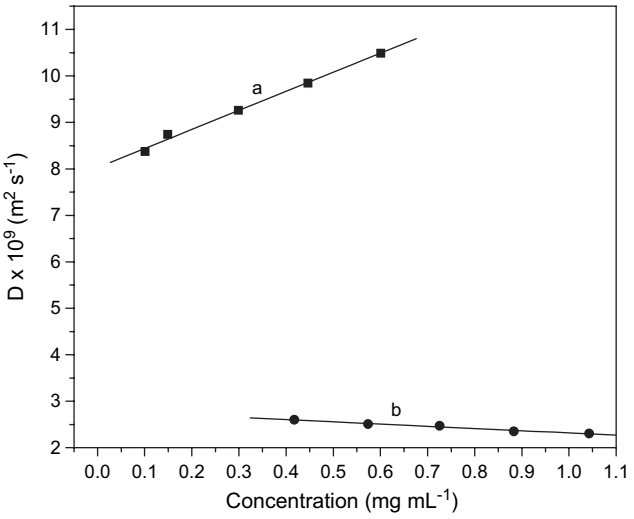

Fig. 10. Plots of D versus concentration of **IV** at 25 °C: (a) in unbuffered distilled water and (b) at pH 3.

in unbuffered distilled water and $D_0 = 2.8 \times 10^{-12}$ m^2 s^{-1} at pH 3 (Table 2). From the Stoke–Einstein equation $R_h = 31$ nm in unbuffered distilled water and $R_h = 88$ nm at pH 3 (Table 2) because the polymer chains are highly stretched due to the repulsion among the positively charged segment.

3.6. Static light scattering (SLS)

The weight-average molecular weight (M_w), the second virial coefficient (A_2) and the z-average radius of gyration (R_g) could be obtained using the Zimm plot relationship:

$$\frac{KC}{R_\theta} = \frac{1}{M_w}\left[1 + \frac{16\pi^2 n^2 \left\langle R_g^2 \right\rangle \sin^2\left(\frac{\theta}{2}\right)}{3\lambda^2}\right] + 2A_2C$$

where the Rayleigh ratio, $R_\theta = (I_s r^2/I_i \sin\theta)$, $K = [4\pi^2 n^2 (\partial n/\partial C)^2/(N_A \lambda^4)]$; C is the concentration of the polymer solution; n is the refractive index of the solvent; θ is the angle of measurement; λ is the wavelength of laser light; N_A is Avogadro's constant; and $(\partial n/\partial C)$ is the refractive index increment of the polymer solution. A plot of (KC/R_θ) versus $[\sin^2(\theta/2) + kC]$ (where k is a plotting constant) can be used to determine the molecular parameters. By extrapolating the data to zero angle and concentration, R_g and A_2 can be obtained from the respective slopes, and the intercepts yield the inverse of the M_w.

For the aqueous solution of (**IV**), the Zimm plots in unbuffered distilled water ($dn/dC = 0.1780$ mL g^{-1}) and pH 3 solution ($dn/dC = 0.1752$ mL g^{-1}) are shown in Fig. 11(a) and (b),

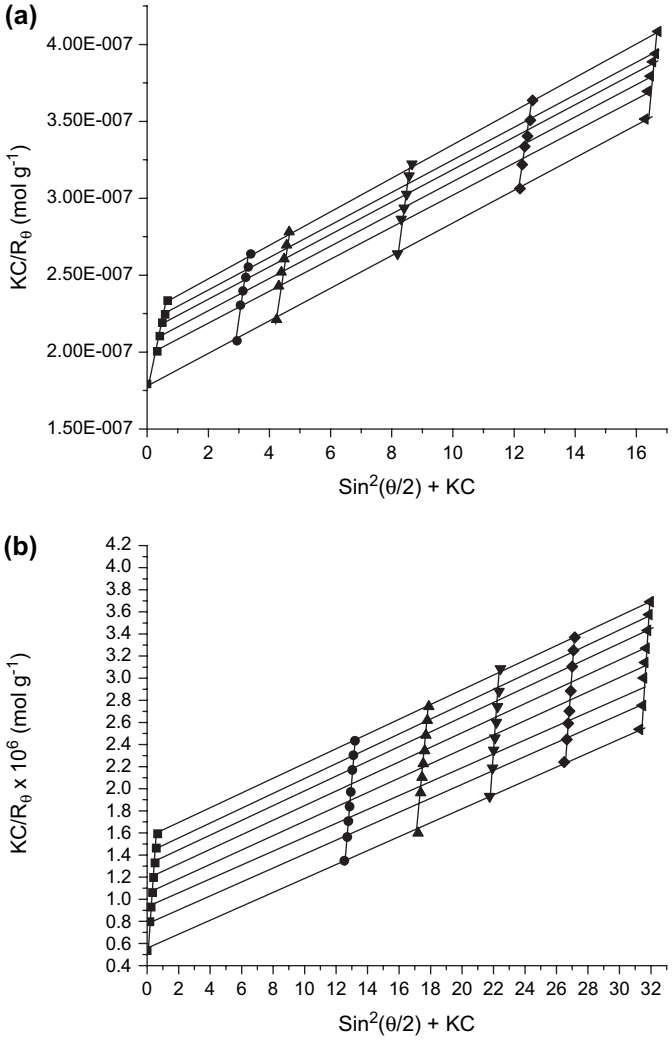

Fig. 11. Zimm plots for **IV** at 25 °C: (a) in unbuffered distilled water and (b) at pH 3.

respectively. The aggregation number (N_{agg}) was calculated to be 242 in unbuffered distilled water and 81 in pH 3 aqueous solution. R_g and R_h of the aggregates are smaller in unbuffered distilled water than those in pH 3 but N_{agg} is larger in distilled water (Table 2). The corresponding R_g/R_h are 1.1 and 0.73, respectively. For uniform sphere, $R_g/R_h = 0.775$ [17], so the micelles at pH 3 are more spherical than in unbuffered distilled water probably due to the stretching of protonated poly(DMAEMA) chains. The polymer–solvent interaction was better in pH 3 than in unbuffered distilled water as indicated by its more positive A_2 value. The aggregates of (**IV**) in unbuffered distilled water and pH 3 are proposed to have the core–shell micellar structures as depicted in Scheme 2.

Table 2
LLS results of (**IV**) in distilled water and at pH 3

	$M_w \times 10^{-6}$ (g mol^{-1})	$A_2 \times 10^4$ (cm^3 mol g^{-2})	$D_0 \times 10^9$ (m^2 s^{-1})	R_g (nm)	R_h (nm)	N_{agg}	R_g/R_h
Unbuffered distilled water	5.58	1.65	8.0	33.7	30.5	242	1.1
pH 3	1.87	9.76	2.8	64.0	87.6	81	0.73

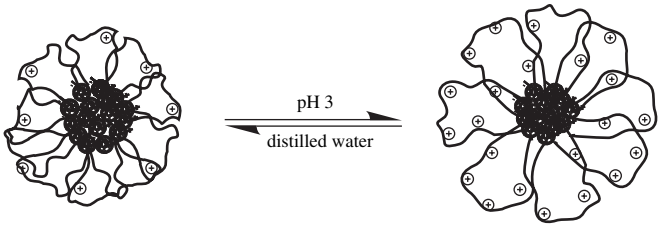

Scheme 2. Proposed micellar structures of IV in unbuffered distilled water and at pH 3.

3.7. Atomic force microscopy (AFM)

Fig. 12(a) and (b) shows the AFM micrographs of (**IV**) aggregates prepared from its aqueous solution. Isolated spherical particles were observed with an average diameter of 40–50 nm. This is slightly smaller than the R_h value obtained by LLS, possibly due to the slight shrinkage of the particles upon drying. As C_{60} is thermally stable up to 600 °C under N_2 atmosphere, after calcinations at 500 °C, the (**IV**) should only be left with C_{60} residue. The AFM micrographs obtained after calcinations for 5 min at 500 °C (Fig. 13(a) and (b)) show clearly that the size of the remaining C_{60} core is about 15–20 nm in diameter.

4. Conclusion

A well-defined water-soluble polymer (**II**) was synthesized via ATRP. C_{60} was successfully incorporated at both ends of the polymer chain via azido cycloaddition. TGA and

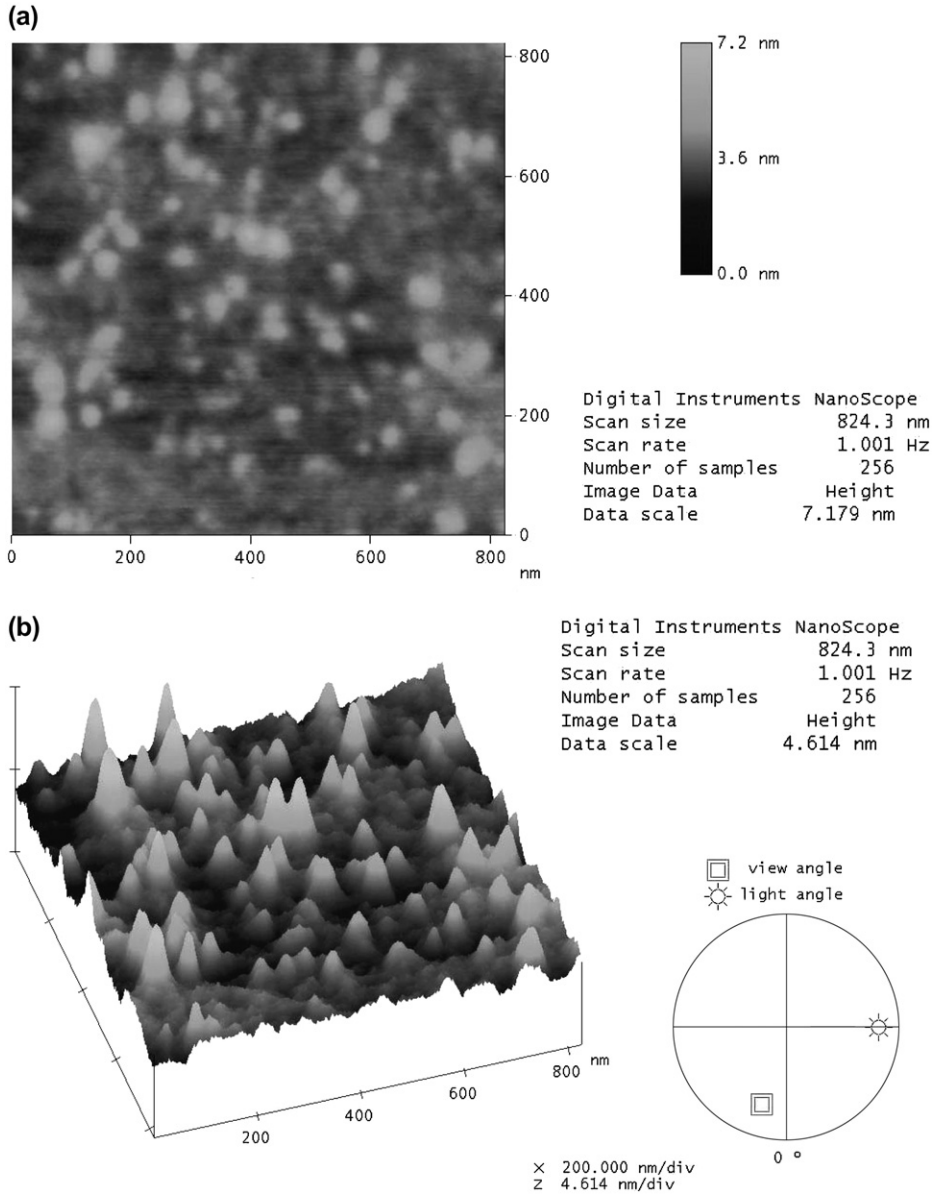

Fig. 12. AFM micrographs of (**IV**) prepared from aqueous solution: (a) height and (b) 3D of height.

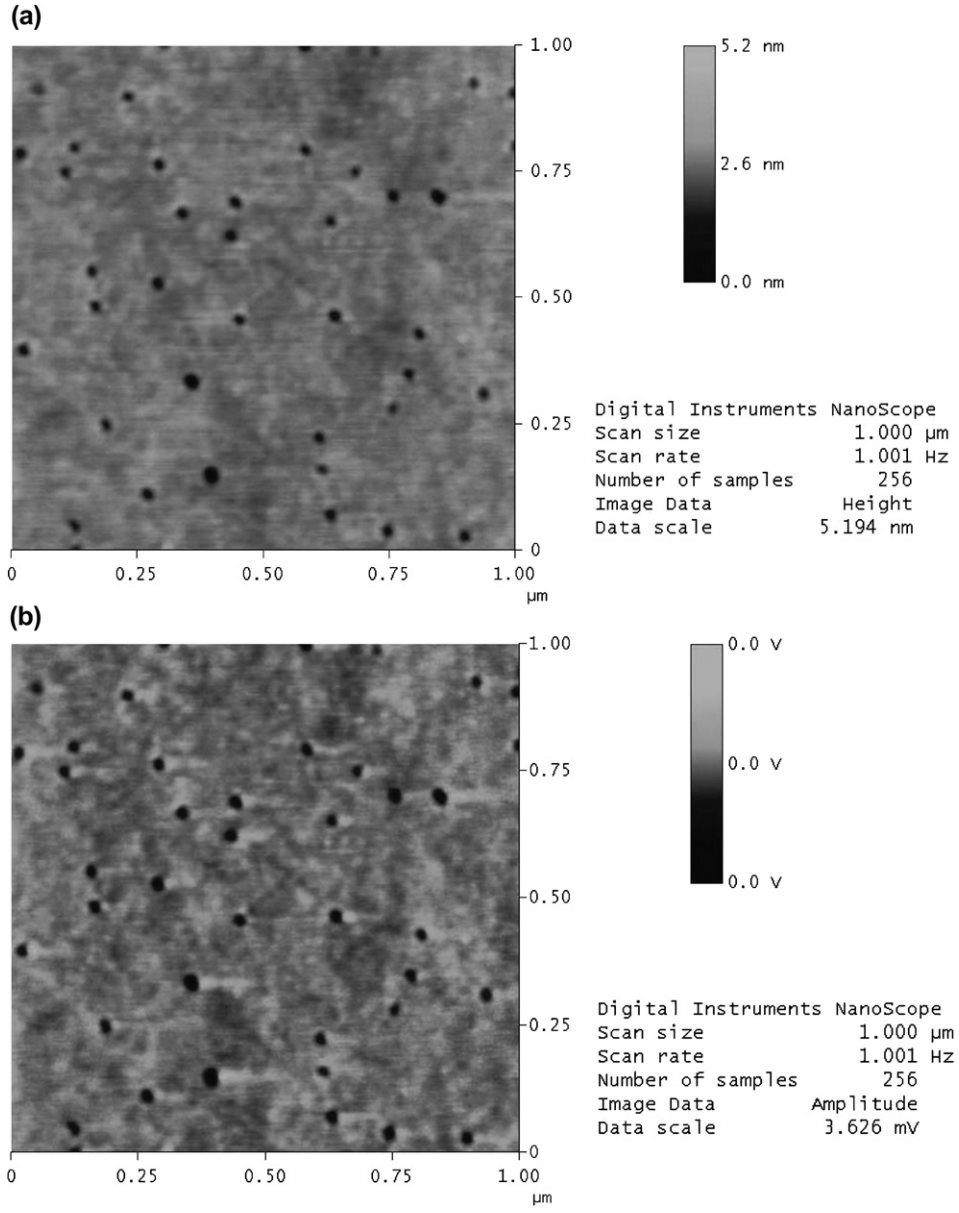

Fig. 13. AFM images of (**IV**) prepared from its aqueous solution after calcinations at 500 °C for 5 min: (a) height and (b) amplitude.

spectroscopic analysis indicated that monocycloaddition to C_{60} had occurred. In aqueous solution, (**IV**) aggregates to form micelles with low CMC values of 28.6 mg dm^{-3} in distilled water and 176.8 mg dm^{-3} at pH 3. The micelles are highly stretched in acidic solution, caused by the repulsion of positive charges among the protonated DMAEMA segments. The micellar size determined by LLS in aqueous solutions was supported by AFM results. Well-separated nanoparticles of C_{60} aggregates were obtained after calcination.

Acknowledgements

This research is funded by the academic fund, National Institute of Education (NIE), Nanyang Technological University, RI 9/03. HY thanks NIE for the postgraduate research scholarship.

Appendix A. Supplementary data

Supplementary data associated with this article can be found in the online version, at doi:10.1016/j.polymer.2007.02.050.

References

[1] Hebard AF, Rosseninsky MJ, Haddon RC, Murphy DW, Glarum SH, Palstra TT, et al. Nature 1991;350:600.
[2] Stephens PW, Cox D, Lauher JW, Mihaly L, Wiley JB, Allemand PM, et al. Nature 1992;335:331.
[3] Jehoulet C, Bard AJ, Wudl F. J Am Chem Soc 1991;113:5456.
[4] Dubois D, Moninot G, Kutner W, Jones MT, Kadish KJ. Phys Chem 1992;96:7137.
[5] Matyjaszewski K, Xia J. Chem Rev 2001;101:2921.

[6] Zhou P, Chen G, Hong H, Du F, Li Z, Li F. Macromolecules 2000; 33:1948.
[7] Li L, Wang C, Long Z, Fu S. J Polym Sci Part A Polym Chem 2000; 38:4519.
[8] Yang J, Li L, Wang C. Macromolecules 2003;36:6060.
[9] Dai S, Ravi P, Tan CH, Tam KC. Langmuir 2004;20:8569.
[10] Tan CH, Ravi P, Dai S, Tam KC. Langmuir 2004;20:9901.
[11] Tan CH, Ravi P, Dai S, Tam KC, Gan LH. Langmuir 2004;20:9882.
[12] Song T, Dai S, Tam KC, Lee SY, Goh SH. Langmuir 2003;19:4798.
[13] Yu H, Gan LH, Hu X, Venkatraman SS, Tam KC, Gan YY. Macromolecules 2005;38:9889.
[14] Wang M, Pramoda KP, Goh SH. Chem Mater 2004;16:3452.
[15] Mao B, Gan LH, Gan YY, Li XS, Ravi P, Tam KC. J Polym Sci Part A Polym Chem 2004;42:5161.
[16] Huang XD, Goh SH, Lee SY. Macromol Chem Phys 2000;201:2660.
[17] Konishi T, Yoshizaki T, Yamakawa H. Macromolecules 1991;24:5614.